

Determination of band alignment between GaO_x and boron doped diamond for a selective-area-doped termination structure

Qi-Liang Wang(王启亮), Shi-Yang Fu(付诗洋), Si-Han He(何思翰), Hai-Bo Zhang(张海波),Shao-Heng Cheng(成绍恒), Liu-An Li(李柳暗), and Hong-Dong Li(李红东)

Citation: Chin. Phys. B, 2022, 31 (**8**): 088104. DOI: 10.1088/1674-1056/ac464e
Journal homepage: http://cpb.iphy.ac.cn; http://iopscience.iop.org/cpb

What follows is a list of articles you may be interested in

Synergistic influences of titanium, boron, and oxygen on large-size single-crystal diamond growth at high pressure and high temperature

Guang-Tong Zhou(周广通), Yu-Hu Mu(穆玉虎), Yuan-Wen Song(宋元文), Zhuang-Fei Zhang(张壮飞), Yue-Wen Zhang(张跃文), Wei-Xia Shen(沈维霞), Qian-Qian Wang(王倩倩), Biao Wan(万彪), Chao Fang(房超), Liang-Chao Chen(陈良超), Ya-Dong Li(李亚东), and Xiao-Peng Jia(贾晓鹏)

Chin. Phys. B, 2022, 31 (**6**): 068103. DOI: 10.1088/1674-1056/ac4650

A low-dimensional crystal growth model on an isotropic and quasi-free sustained substrate

Chenxi Lu(卢晨曦), Senjiang Yu(余森江), Lingwei Li(李领伟), Bo Yang(杨波), Xiangming Tao(陶向明), Gaoxiang Ye(叶高翔)

Chin. Phys. B, 2020, 29 (**3**): 038101. DOI: 10.1088/1674-1056/ab6968

Band offset and electronic properties at semipolar plane AlN(1101)/diamond heterointerface

Kong-Ping Wu(吴孔平), Wen-Fei Ma(马文飞), Chang-Xu Sun(孙昌旭), Chang-Zhao Chen(陈昌兆), Liu-Yi Ling(凌六一), Zhong-Gen Wang(王仲根)

Chin. Phys. B, 2018, 27 (**5**): 058101. DOI: 10.1088/1674-1056/27/5/058101

Energy-band alignment of atomic layer deposited $(HfO_2)_x(Al_2O_3)_{1-x}$ gate dielectrics on 4H-SiC

Jia Ren-Xu, Dong Lin-Peng, Niu Ying-Xi, Li Cheng-Zhan, Song Qing-Wen, Tang Xiao-Yan, Yang Fei, Zhang Yu-Ming

Chin. Phys. B, 2015, 24 (**3**): 038103. DOI: 10.1088/1674-1056/24/3/038103

White electroluminescence of n-ZnO：Al/p-diamond heterostructure devices

Yang Can, Wang Xiao-Ping, Wang Li-Jun, Pan Xiu-Fang, Li Song-Kun, Jing Long-Wei

Chin. Phys. B, 2013, 22 (**8**): 088101. DOI: 10.1088/1674-1056/22/8/088101

Determination of band alignment between GaO_x and boron doped diamond for a selective-area-doped termination structure

Qi-Liang Wang(王启亮)[1,2], Shi-Yang Fu(付诗洋)[1], Si-Han He(何思翰)[1], Hai-Bo Zhang(张海波)[3], Shao-Heng Cheng(成绍恒)[1,2,†], Liu-An Li(李柳暗)[1,2,‡], and Hong-Dong Li(李红东)[1,2]

[1] *State Key Laboratory of Superhard Materials, Jilin University, Changchun* 130012, *China*
[2] *Shenzhen Research Institute, Jilin University, Shenzhen* 518057, *China*
[3] *Guangdong Juxin New Material Technology Co., Ltd, Zhuhai* 519000, *China*

(Received 14 September 2021; revised manuscript received 13 December 2021; accepted manuscript online 24 December 2021)

An n-GaO_x thin film is deposited on a single-crystal boron-doped diamond by RF magnetron sputtering to form the pn heterojunction. The n-GaO_x thin film presents a small surface roughness and a large optical band gap of 4.85 eV. In addition, the band alignment is measured using x-ray photoelectron spectroscopy to evaluate the heterojunction properties. The GaO_x/diamond heterojunction shows a type-II staggered band configuration, where the valence and conduction band offsets are 1.28 eV and 1.93 eV, respectively. These results confirm the feasibility of the use of n-GaO_x as a termination structure for diamond power devices.

Keywords: GaO_x, boron-doped diamond, edge termination, band alignment

PACS: 81.05.ug, 85.30.Kk, 84.30.Jc, 71.20.–b **DOI:** 10.1088/1674-1056/ac464e

1. Introduction

Diamond is a promising material for next-generation-power electronic and optoelectronic device applications due to its excellent physical and electrical properties.[1–3] The extremely large critical breakdown field (10 MV/cm), high thermal conductivity (22 W/cm·K) and high carrier mobility (2200 $cm^2 \cdot V^{-1} \cdot s^{-1}$ and 1800 $cm^2 \cdot V^{-1} \cdot s^{-1}$ for electrons and holes, respectively) are beneficial to achieve a high Baliga's figure of merit (BFOM). The p-type boron-doped diamond-based power rectifiers, including both Schottky barrier diodes (SBD) and PN diodes (PND), have attracted considerable attentions.[4] The SBD presents a typically low on-state voltage and no storage of minority carriers, which is a promising structure for high-efficiency rectifier application. However, the device's performances, especially the breakdown electric field, are still far below the theoretical limit of diamond, which can be ascribed to the material quality, non-optimized device design, termination structure and so on. It was reported that the field-crowding effect at the junction periphery under a large reverse voltage increases the leakage current and leads to a reduced breakdown voltage. Recently, different kinds of termination structures have been proposed for diamond SBDs. Diamond Schottky-pn diodes (SPNDs) with a lightly nitrogen-doped layer realized a high forward current density of over 20 kA/cm^2 at 7 V and a high breakdown electric field of 3.3 MV/cm at room temperature.[5] Using boron implanted guard ring termination, the average breakdown voltage of the device with a 310 nm p^- drift layer was significantly improved from 79 V to 125 V.[6] Using a floating metal guard ring structure, an SBD device with a breakdown electric field of 2.6 MV/cm was also fabricated.[7]

Generally, high-power switching devices encounter a trade-off between two contradicting properties, namely, high blocking voltage and low forward loss. From this point, the edge termination (ET, Fig. 1(a)) and junction barrier Schottky (JBS, Fig. 1(b)) diode, combining the Schottky contact with an area-selective pn-junction, are enable to benefit from both.[8,9] In the forward bias region, a Schottky contact with a low Schottky barrier height metal can realize small forward losses, while the lateral field of a buried pn-junction helps to shield the strong electric fields around the Schottky contact under high reverse bias. However, although p-type doping can be easily realized using a boron dopant,[10] effective n-type doping is still a challenge for diamond due to the large activation energy (e.g., 1.7 eV for nitrogen) or low doping efficiency (e.g., 50%–90% compensation ratio for phosphorus-doped (001) diamond).[11] In addition, the ion implantation technique degrades the crystalline quality and needs high temperature annealing.[12]

Alternatively, gallium oxide (GaO_x), with a wide bandgap of approximately 4.8 eV, a high critical electrical field of 8 MV/cm and large BFOM is suitable for high-power applications.[13] Furthermore, GaO_x can obtain n-type doping easily with electron concentration ranges from 10^{16} cm^{-3}–10^{19} cm^{-3}. The structure, morphology and optical properties of GaO_x thin films can be adjusted by the growth conditions during magnetron sputtering deposition, which enable the selective area deposition of n-type regions with easy

†Corresponding author. E-mail: chengshaoheng@jlu.edu.cn
‡Corresponding author. E-mail: liliuan@jlu.edu.cn

© 2022 Chinese Physical Society and IOP Publishing Ltd

controllability.[14] Previously, an n-GaO_x/p-diamond heterojunction photodiode was demonstrated with a high rectification ratio and low reverse leakage current, which is beneficial to obtain high responsivity, a high photo-to-dark-current ratio, and fast response time due to the built-in electric field.[15] For power diodes, by introducing the GaO_x/diamond pn-heterojunction, a depletion region with extra ionized charge attracts the electric field, which is beneficial to shield the field-crowding effect.[16] However, the fabrication of diamond diodes with ET and/or JBS using n-GaO_x has not been extensively investigated. The oxide materials are usually used as gate dielectrics for semiconductor devices. Generally, the interface band offsets between the gate dielectric play a key role in device operation, which determines the mobility and transport properties, as well as the threshold voltage stability.[17] In addition, the band offsets are essential to predict the carrier barrier for pn heterojunction applications, which affects both the forward turn-on and reverse depletion region. Therefore, it is very important to measure the band offsets at the interfaces of oxides and semiconductors.[18,19]

In this report, GaO_x thin films are deposited on a single-crystal boron-doped diamond by RF magnetron sputtering to form a heterojunction. In addition, the band offsets and band configuration at the n-GaO_x/p-diamond heterojunction interface are measured using x-ray photoelectron spectroscopy (XPS).

2. Experiment

The p-type single crystalline boron-doped diamond (BDD) was grown on a single-crystal seed using the microwave plasma chemical vapor deposition system. The type-Ib (100) seeds were commercially available with a dimension of 3 mm × 3 mm × 1 mm. During growth, H_2/CH_4/boron flow rates of 200/2/4 sccm were adopted in the chamber to reach a reactor pressure of approximately 8 kPa. To realize p-type doping, liquid $B(OCH_3)_3$ (kept at 25 °C) was chosen as the boron dopant. The $B(OCH_3)_3$ was carried by bubbling H_2 with a flow rate of 4 sccm. The thickness of the p-diamond layer was approximately 1 μm when the growth duration was adjusted to 30 min. The electrical properties of the BDD were examined using Hall-effect measurements. The hole concentration and mobility of the sample were approximately 1.39×10^{19} cm^{-3} and 30.4 $cm^2 \cdot V^{-1} \cdot s^{-1}$, respectively.

To determine the band discontinuities at the GaO_x/diamond interface, diamond samples with 4 nm and 40 nm-thick GaO_x were deposited by radio frequency magnetron sputtering (as shown in Fig. 1(c)). The deposition conditions of GaO_x were similar to previous work.[14] After growth, the boron-doped diamond samples were treated by H_2SO_4:H_2O_2 (3:1) solution and organic cleaning to form an oxygen termination. The GaO_x target (99.99% purity) was employed above the diamond substrate with a spacing of 10 cm. The oxygen and argon gas mixture, with a flow rate of 2 sccm and 40 sccm, was introduced during deposition. The sputtering power and growth ratio were 160 W and 0.33 nm/min, respectively. The GaO_x thin film presents a (201) texture with a bandgap of approximately 5.0 eV deduced using the Tauc method.[14]

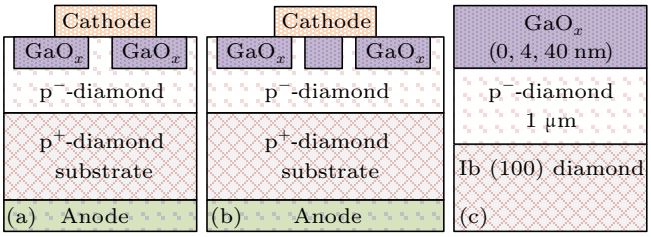


Fig. 1. A schematic view of the vertical diamond diode with GaO_x edge termination (a) and junction barrier Schottky (b) structures. (c) The samples for XPS measurements.

The XPS apparatus (Thermo Fisher Scientific) was calibrated before measurements by C 1s with a binding energy at approximately 284.80 ± 0.08 eV. A monochromatized Al $K\alpha$ (1486.6 ± 0.08 eV) was chosen as the radiation source with a spot size of approximately 500 μm. The standard deviations of the core level energy and valence band are ±0.08 eV and ±0.2 eV, respectively. Based on the extensively adopted Kraut method,[20–22] the valence band offset (VBO, ΔE_V) can be calculated from the formula

$$\Delta E_V = \left(E_{Ga2p}^{GaO_x} - E_{VBM}^{GaO_x}\right) - \left(E_{C1s}^{Diamond} - E_{VBM}^{Diamond}\right) - \Delta E_{CL}, \quad (1)$$

where $E_{Ga2p}^{GaO_x}$ and $E_{VBM}^{GaO_x}$ are the Ga 2p energy and valence band maximum (VBM) of the bulk GaO_x, respectively. Here, $E_{C1s}^{Diamond}$ and $E_{VBM}^{Diamond}$ are C 1s energy and the VBM of the diamond substrate, respectively, while $\Delta E_{CL} = (E_{Ga2p}^{GaO_x} - E_{C1s}^{Diamond})$ is the core level energy difference of the GaO_x/diamond interface. Then, with the band gap values of GaO_x and diamond, the conduction-band offset (CBO, ΔE_c) can be deduced from

$$\Delta E_c = \Delta E_V + E_g^{Diamond} - E_g^{GaO_x}. \quad (2)$$

3. Results and discussion

Firstly, the crystalline quality of BDD and GaO_x (40 nm) films is evaluated using an x-ray diffraction system (XRD, Rigaku D/MAX-RA with Cu $K\alpha$ radiation). For the diamond, only a strong peak appears at approximately 119.7°, which can be assigned to the diffraction of the (004) crystal plane (Fig. 2(a)). However, there are no obvious peaks that can be assigned to the GaO_x film (Fig. 2(b)), implying the amorphous structure of the sputtered film on diamond. The surface

morphologies of the BDD and GaO_x films are characterized at three different positions using an atomic force microscope (AFM, Bruker Dimension Edge). The scan dimension is set to 5 μm × 5 μm with a tapping-mode. The typical morphologies measured at the in the central area are shown in the insets of Fig. 2. It demonstrates that the BDD surface presents many small pits with a root mean square roughness (RMS) of 0.83 nm (insets of Fig. 2(a)), which may be ascribed to the acid solution treatment. As shown in Fig. 2(b), the surface RMS is approximately 0.71 nm after the deposition of GaO_x film (40 nm).

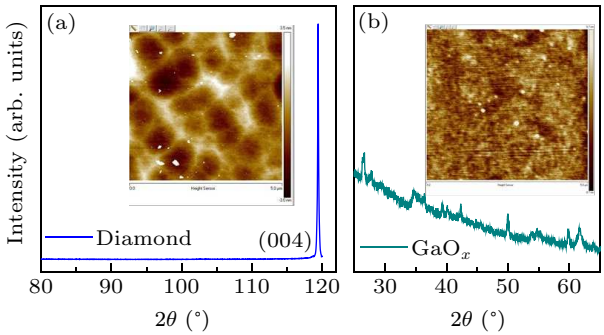


Fig. 2. AFM images of BDD (a) and GaO_x (b) films scanned in 5 μm × 5 μm.

The crystalline quality of BDD is also evaluated using Raman spectroscopy (Renishaw inVia Raman microscope, using a 514-nm Ar^+ laser as the excitation source). As shown in Fig. 3(a), only a sharp peak around 1333 cm^{-1} is observed in the spectrum, implying high purity, and the non-diamond (or sp^2) phase is almost eliminated. Moreover, Fano interference as well as the broad satellite peaks (around 480 cm^{-1} and 1190 cm^{-1}) are not obvious.[23] The bandgap energy (E_g) of the GaO_x film on diamond is an important parameter used to calculate the conduction band offset (ΔE_c). From the photoelectron energy loss peak on the O 1s core-level spectrum of the GaO_x bulk sample (as shown in Fig. 3(b)), the E_g is deduced from the energy difference between the O 1s core level and the threshold energy of the photoelectron energy loss peak. The threshold energy is determined to be 537.00 ± 0.08 eV by extrapolating a linear fit of the leading edge for the photoelectron energy loss peak to the baseline.[24] Then, the E_g is calculated to be approximately 4.85 ± 0.08 eV.

The SEM images of the diamond sample coated with 4 nm GaO_x are shown in Fig. 4(a). It is observed that the diamond surface is fully covered by the GaO_x. In addition, the element (O and Ga) scanning in Figs. 4(b) and 4(c) indicates good uniformity. To calculate the energy difference of $(E_{C1s}^{Diamond} - E_{VBM}^{Diamond})$, we record the C 1s core-level spectrum and the VBM of the bulk BDD (Fig. 5). The VBM of diamond is deduced to be approximately 1.63 ± 0.2 eV. The relatively larger VBM value than the active energy of boron (approximately 0.37 eV) indicates that the doping concentration is relatively lower, which is consistent with the Raman results. Furthermore, the C 1s spectrum can be fitted into three peaks, including the C–Si (central at 283.23 ± 0.08 eV), C–C (central at 284.84 ± 0.08 eV) and C–H (central at 285.97 ± 0.08 eV) bonding.[25,26] In the survey spectrum of the diamond film (not shown), a small Si signal was detected with an element percentage of approximately 4.3%. The C–Si bonding possibly originates from the surface contamination because the sample is kept in ambient atmosphere before the XPS measurement. Then, we can obtain the energy difference of $(E_{C1s}^{Diamond} - E_{VBM}^{Diamond})$, which is approximately 283.21 ± 0.2 eV.[27]

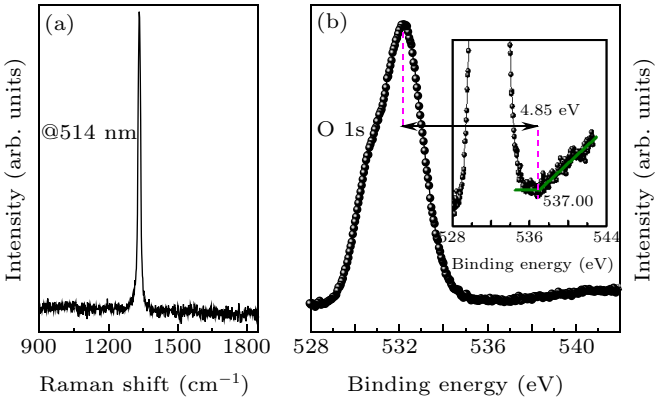


Fig. 3. The Raman spectroscopy of the film excited by a 514 nm laser (a), and the O 1s core-level spectrum of GaO_x (b). The inset is the photoelectron energy loss peak used to determine the bandgap.

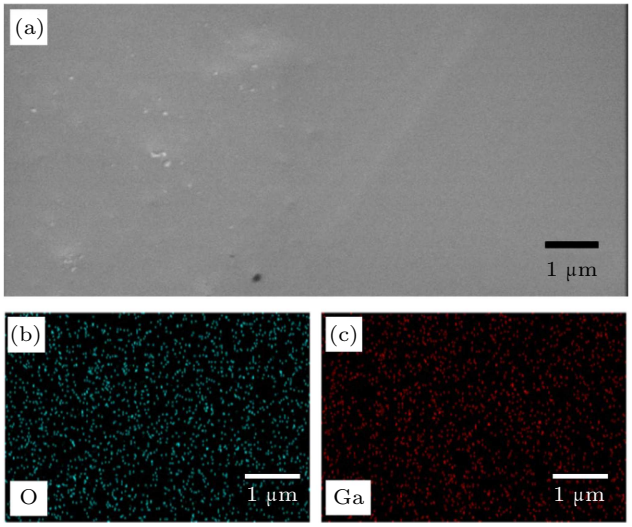


Fig. 4. The surface morphology (a) and the corresponding elements distributions [(b) and (c)] of the diamond coated with 4 nm GaO_x.

Similarly, the energy difference of $(E_{Ga2p}^{GaO_x} - E_{VBM}^{GaO_x})$ is obtained on the 40 nm thick GaO_x film on BDD substrate (Fig. 6). The VBM of GaO_x is approximately 3.29 ± 0.2 eV, implying that the Fermi level is higher than the middle bandgap and that the GaO_x film presents a weak n-type conductivity. However, this concentration makes it difficult to realize good ohmic contact for Hall measurement and device fabrication. In the future, intentional doping by adding Si or Sn into the GaO_x target is needed to improve the conductivity. The Ga 2p core-level spectrum is dominated by the peak

central at 1118.41 ± 0.08 eV. Besides, the corresponding O 1s spectrum is well fitted by two contributions (inset of Fig. 6). The peaks at nearly 530.59 ± 0.08 eV and 532.21 ± 0.08 eV are attributed to O–Ga (GaO_x) and OH–Ga bonds ($Ga(OH)_3$), respectively. This result indicates that a certain number of OH-groups exist on the surface of GaO_x because the sample is kept in ambient atmosphere before XPS measurement. Then, we can obtain the energy difference of $(E_{Ga2p}^{GaO_x} - E_{VBM}^{GaO_x})$, which is approximately 1115.12 ± 0.2 eV.

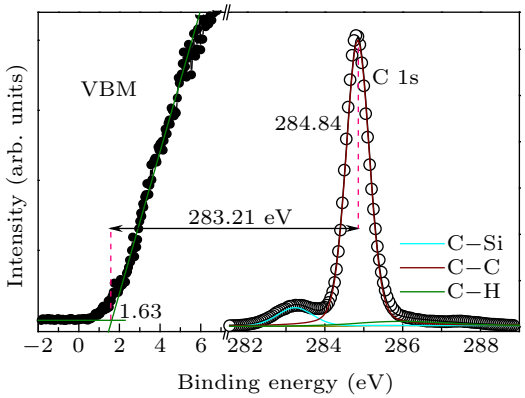


Fig. 5. The valence band and the C 1s spectrum of bulk BDD. The energy difference $(E_{C1s}^{Diamond} - E_{VBM}^{Diamond})$ is calculated to be 283.21 ± 0.2 eV by fitting the curves.

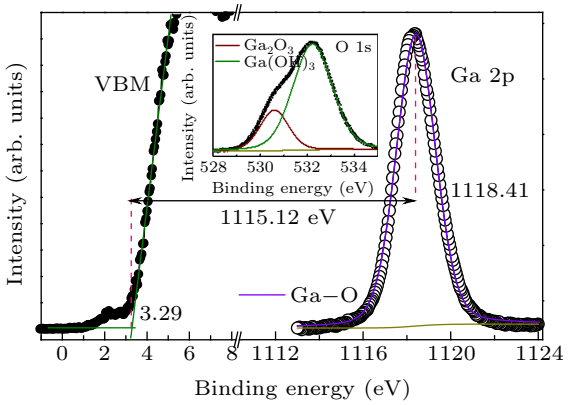


Fig. 6. The valence band and C 1s spectra of the bulk GaO_x on diamond. The energy difference of $(E_{Ga2p}^{GaO_x} - E_{VBM}^{GaO_x})$ is calculated to be 1115.12 ± 0.2 eV by fitting the curves.

Finally, a thin layer of 4 nm GaO_x was deposited on the BDD surface to determine the energy difference of $(E_{Ga2p}^{GaO_x} - E_{C1s}^{Diamond})$. Obviously, both C 1s signals from boron-doped diamond and a Ga 2p signal from thin GaO_x are detected (Fig. 7). Compared with the bulk diamond material, peaks in the C 1s core-level curve shift to approximately 284.75 ± 0.08 eV, 285.87 ± 0.08 eV, and 288.95 ± 0.08 eV, corresponding to the C–C, C–H, and C–O bonds, respectively. During the sputtering of GaO_x, the oxygen atom at the diamond/GaO_x interface will enhance the intensity of the C–O peak. On the other hand, the Ga 2p core-level spectrum is nearly the same as that of the thick GaO_x, except that the peak slightly shifts to approximately 1117.94 ± 0.08 eV. However, the corresponding O 1s spectrum of the thin GaO_x shows an obvious change, as shown in the inset of Fig. 6. Together with the O–Ga (GaO_x) and OH–Ga ($Ga(OH)_3$) peaks at nearly 530.63 ± 0.08 eV and 532.43 ± 0.08 eV, a new O–C peak at central at around 531.57 ± 0.08 eV was observed.[28] This result is also consistent with the C 1s spectrum. Therefore, the energy difference $(E_{Ga2p}^{GaO_x} - E_{C1s}^{Diamond})$ of 833.19 ± 0.08 eV is calculated based on the fitting results.

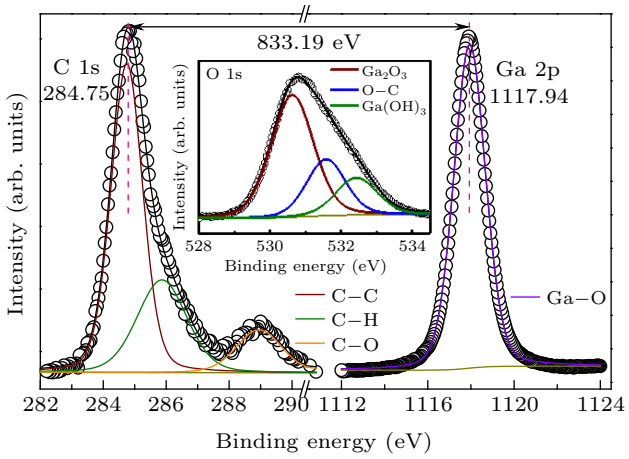


Fig. 7. The C 1s and Ga 2p spectrum for the 4 nm GaO_x-coated diamond. The corresponding $(E_{Ga2p}^{GaO_x} - E_{C1s}^{Diamond})$ is deduced to be 833.19 ± 0.08 eV.

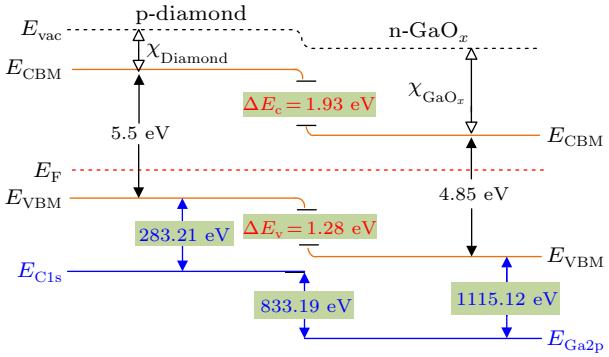


Fig. 8. The band configuration of the GaO_x/diamond pn heterojunction based on the XPS results.

Table 1 summarizes the fitting results of the XPS and the corresponding energy difference; the ΔE_V between GaO_x and diamond is calculated to be 1.28 ± 0.2 eV according to Eq. (1). Using the room temperature band gaps of GaO_x and diamond (5.50 eV), we can calculate the ΔE_c of approximately 1.93 ± 0.2 eV. The band structure in the GaO_x/diamond interface is a type-II straddling band configuration, as shown in Fig. 8. In addition, Table 2 summarizes the band alignments between diamond and other materials reported in previous works for comparison. Both the electron and hole can contribute in the conduction without accumulation in the type-II staggered band configuration, which helps to decrease the on-resistance and power loss. It is worth noting that the ΔE_V calculated from the VBM discrepancy should be 1.66 ± 0.2 eV, implying that some effects decrease the ΔE_V of 0.38 ± 0.2 eV at the interface. It is well known that the adsorption of hydrogen atoms on a diamond surface (C–H bonds) shifts the energy

band of diamond to a negative electron affinity of 1.5 eV.[29] In addition, the C–H generates a high concentration of two-dimensional hole gas (2DHG) on the surface, resulting in upward band bending.[30] Then, the C–H at the interface will increase the band offsets. On the other hand, the adsorption of oxygen atoms (C–O bonds) gives a positive electron affinity of approximately 0.5 eV and turns the surface into nearly insulator, resulting in decreasing band offsets. Therefore, the variation of ΔE_V from the theoretical value is attributed to the increasing C–O at the interface.

Table 1. A summary of the fitting results of XPS and the corresponding energy differences.

Sample	Region	Binding energy (eV)	Energy difference (eV)
Diamond bulk	C 1s	284.84	$(E_{C1S}-E_{VBM})^{Diamond}$
	VBM	1.63	283.21
GaO_x (40 nm)	Ga 2p	1118.41	$(E_{Ga2p}-E_{VBM})^{GaO_x}$
	VBM	3.29	1115.12
GaO_x/diamond	C 1s	284.75	$(E_{Ga2p}-E_{C1S})^{GaO_x/Diamond}$
	Ga 2p	1117.94	833.19

Table 2. A summary of the band alignments between diamond and other materials.

Substrate	Material	VBO (eV)	CBO (eV)	Ref.
BDD	n-GaO	1.28	1.93	this work
BDD	p-NiO	1.07	0.74	[16]
H-diamond	Al_2O_3	3.28	1.88	[31]
H-diamond	HfO_2	2.60	2.70	[32]
Diamond	c-BN	0.80	1.70	[33]

4. Conclusion and perspectives

In conclusion, a GaO_x/diamond pn heterojunction is deposited by RF magnetron sputtering for band alignment measurements. GaO_x thin film deposited on the single-crystal boron-doped diamond presents a small surface roughness of 0.71 nm and a band gap of approximately 4.85 eV. Then, XPS is used to determine the band alignment of the GaO_x/diamond pn heterojunction. The VBM values confirm that the GaO_x and diamond are n- and p-type conduction, respectively. The VBO and CBO are calculated to be 1.28 eV and 1.93 eV, respectively. The variation of ΔE_V from the theoretical value is attributed to the increasing C–O at the interface. By combining the material and interface characteristics, the wide bandgap and the type-II staggered band configuration, the GaO_x/diamond heterojunction is promising for diamond-power electronic device applications.

Acknowledgment

Project supported by the Key-Area Research and Development Program of Guangdong Province, China (Grant No. 2020B0101690001).

References

[1] Lu Y, Lin C and Shan C 2018 *Adv. Opt. Mater.* **6** 1800359
[2] Ekimov E, Sidorov V, Bauer E, *et al.* 2004 *Nature* **428** 542
[3] Gloor S, Lüthy W, Weber H, *et al.* 1999 *Appl. Surf. Sci.* **138-139** 135
[4] Umezawa H 2018 *Mater. Sci. Semicond. Process.* **78** 147
[5] Matsumoto T, Mukose T, Makino T, *et al.* 2017 *Diam. Relat. Mater.* **75** 152
[6] Yu X, Zhou J, Wang Y, *et al.* 2019 *Diam. Relat. Mater.* **92** 146
[7] Driche K, Rugen S, Kaminski N, *et al.* 2018 *Diam. Relat. Mater.* **82** 160
[8] Wang Y, Pu T, Li X, *et al.* 2021 *Mater. Sci. Semicond. Process.* **125** 105628
[9] Kubovic M, El-Hajj H, Butler J, *et al.* 2007 *Diam. Relat. Mater.* **16** 1033
[10] Li L, Li H, Lv X, *et al.* 2010 *Appl. Surf. Sci.* **256** 1764
[11] Matsumoto T, Mukose T, Makino T, *et al.* 2017 *Diam. Relat. Mater.* **75** 152
[12] Das D, Kandasami A and Rao M 2021 *Appl. Phys. Lett.* **118** 102102
[13] Liu Z, Li P, Zhi Y, *et al.* 2019 *Chin. Phys. B* **28** 017105
[14] Li S, Jiao S, Wang D, *et al.* 2018 *J. Alloys Compd.* **753** 186
[15] Kim H, Tarelkin S, Polyakov A, *et al.* 2020 *ECS J. Solid State Sci. Technol.* **9** 045004
[16] Zhang T, Li X, Pu T, *et al.* 2020 *Mater. Sci. Semicond. Process.* **105** 104740
[17] Liu Z, Yu J, Li P, *et al.* 2019 *J. Phys. D: Appl. Phys.* **52** 295104
[18] Sun X, Zhu C, Zhu X, *et al.* 2021 *Adv. Electron. Mater.* **7** 2001174
[19] Lo S, Mirkovic T, Chuang C, *et al.* 2011 *Adv. Mater.* **23** 180
[20] Kraut E, Grant R, Waldrop J, *et al.* 1986 *Phys. Rev. Lett.* **44** 1620
[21] Liu J, Cheng S, Liao M, *et al.* 2013 *Diam. Relat. Mater.* **38** 24
[22] Gonon P, Gheeraert E, Deneuville A, *et al.* 1995 *J. Appl. Phys.* **78** 7059
[23] Bernard M, Deneuville A, Muret P, *et al.* 2004 *Diam. Relat. Mater.* **13** 282
[24] Miyazaki S 2001 *J. Vac. Sci. Technol. B* **19** 2212
[25] Zhang D, Li S, Zuo X, *et al.* 2020 *Diam. Relat. Mater.* **108** 107923
[26] Navas J, Araujo D, Pinero J, *et al.* 2018 *Appl. Surf. Sci.* **433** 408
[27] Kono S, Kageura T, Hayashi Y, *et al.* 2019 *Diamond & Related Materials* **93** 105
[28] Li L, Wang W, He L, *et al.* 2017 *J. Alloys Compd.* **728** 400
[29] Gao Y, Gao N, Li H, *et al.* 2018 *Nanoscale* **10** 15788
[30] Macdonald D, Crawford K, Tallaire A, *et al.* 2018 *IEEE Electron Device Letters* **39** 1354
[31] Ren Z, Lv D, Xu J, *et al.* 2020 *Appl. Phys. Lett.* **116** 013503
[32] Liu J, Liao M, Imura M, *et al.* 2012 *Appl. Phys. Lett.* **101** 252108
[33] Shammas J, Yang Y, Wang X, *et al.* 2017 *Appl. Phys. Lett.* **111** 171604